Effects of magnesium ion on kinetic stability and spin distribution of phenoxyl radical derived from a vitamin E analogue: mechanistic insight into antioxidative hydrogen-transfer reaction of vitamin E †

Ikuo Nakanishi,*[a] Kiyoshi Fukuhara,*[b] Tomokazu Shimada,[b,c] Kei Ohkubo,[d] Yuko Iizuka,[e] Keiko Inami,[e] Masataka Mochizuki,[e] Shiro Urano,[c] Shinobu Itoh,[f] Naoki Miyata[g] and Shunichi Fukuzumi *[d]

[a] *Redox Regulation Research Group, Research Center for Radiation Safety, National Institute of Radiological Sciences, Inage-ku, Chiba 263-8555, Japan. E-mail: nakanis@nirs.go.jp; Fax: +81-43-255-6819; Tel: +81-43-206-3131*
[b] *Division of Organic Chemistry, National Institute of Health Sciences, Setagaya-ku, Tokyo 158-8501, Japan*
[c] *Department of Applied Chemistry, Shibaura Institute of Technology, Minato-ku, Tokyo 108-8548, Japan*
[d] *Department of Material and Life Science, Graduate School of Engineering, Osaka University, CREST, Japan Science and Technology Corporation, Suita, Osaka 565-0871, Japan*
[e] *Division of Organic and Bioorganic Chemistry, Kyoritsu College of Pharmacy, Minato-ku, Tokyo 105-8512, Japan*
[f] *Department of Chemistry, Graduate School of Science, Osaka City University, Sumiyoshi-ku, Osaka 558-8585, Japan*
[g] *Department of Organic and Medicinal Chemistry, Graduate School of Pharmaceutical Sciences, Nagoya City University, Mizuho-ku, Nagoya 467-8603, Japan*

The phenoxyl radical $1^{\bullet}$ of a vitamin E analogue, generated by the reaction of 2,2,5,7,8-pentamethylchroman-6-ol (**1H**) with 2,2-di(4-*tert*-octylphenyl)-1-picrylhydrazyl (DPPH$^{\bullet}$) or galvinoxyl (G$^{\bullet}$), was significantly stabilized by the presence of Mg^{2+}. Addition of Mg^{2+} into a solution of $1^{\bullet}$ resulted in a red shift of the absorption band of $1^{\bullet}$ as well as a decrease in the g value of the EPR spectrum of $1^{\bullet}$, indicating a complex formation between $1^{\bullet}$ and Mg^{2+}. The complexation between the phenoxyl radical and Mg^{2+} significantly retards the disproportionation reaction of $1^{\bullet}$ by electronic repulsion between the metal cation and a generated organic cation (1^{+}), leading to stabilization of the organic radical species. No effect of Mg^{2+} on the rate of hydrogen atom transfer from **1H** to DPPH$^{\bullet}$ or to G$^{\bullet}$ was observed, suggesting that the hydrogen-transfer reaction between **1H** and DPPH$^{\bullet}$ or G$^{\bullet}$ proceeds *via* a one-step hydrogen atom transfer mechanism rather than electron-transfer followed by proton transfer.

Introduction

Vitamin E (α-tocopherol, α-TOH) is a very effective biological antioxidant that can scavenge peroxyl radicals in biological membranes, preventing oxidative injury by toxic and carcinogenic chemicals.[1–3] It has been suggested that α-TOH traps radicals by hydrogen atom transfer from its phenolic OH group to form the corresponding phenoxyl radical species, α-TO$^{\bullet}$,[1–3] which readily decomposes, leading to a wide variety of oxidation products of α-tocopherol.[4–21] However, very little is known about the elementary steps of the oxidation reaction of α-TOH. There are two possibilities in the mechanisms of oxidation reactions, *i.e.*, a one-step hydrogen atom transfer or electron transfer followed by proton transfer.[22–24] Svanholm *et al.* have proposed that a first step in the antioxidative activity of tocopherol produces a cation radical by one electron extraction.[25] On the other hand, Burton and Ingold have reported that the

reaction of α-TOH with peroxyls exhibits a substantial deuterium kinetic isotope effect ($k_H/k_D = 5.4 \pm 0.4$), indicating that the hydrogen atom transfer is rate controlling.[26] Mukai *et al.* have also demonstrated that the antioxidant activity of tocopherol compounds relates to the total electron-donating character of the alkyl group substituents on the aromatic ring.[27] Thus, it is still not clear whether the hydrogen-transfer reaction of α-TOH proceeds *via* a one-step hydrogen transfer or electron transfer followed by proton transfer. It has been reported that the effect of Mg^{2+} on the hydrogen-transfer rates from NADH (dihydronicotinamide adenine dinucleotide) analogues to aminoxyl or nitrogen radicals provides a reliable criterion for distinguishing between the one-step hydrogen atom transfer and the electron-transfer mechanisms.[28] It has also been demonstrated that metal ions such as Mg^{2+} and Ca^{2+} can stabilize phenoxyl radicals by forming complexes.[29] In this context, the effects of metal ions on the oxidation reaction of α-TOH would be of significant interest to elucidate the mechanistic aspect of the antioxidative reactions of vitamin E.

We report herein that a phenoxyl radical ($1^{\bullet}$) of a vitamin E analogue, 2,2,5,7,8-pentamethylchroman-6-ol (**1H**), generated

---

DOI: 10.1039/b205380b

in the reaction of **1H** with 2,2-di(4-*tert*-octylphenyl)-1-picryl-hydrazyl (DPPH$^\bullet$) or galvinoxyl (G$^\bullet$) is significantly stabilized by interaction with Mg^{2+}. The electronic structure of the Mg^{2+}–**1$^\bullet$** complex thus generated has been well characterized by EPR. Detailed spectroscopic and kinetic analyses on the **1H**–DPPH$^\bullet$ (G$^\bullet$)–Mg^{2+} system provide a valuable insight into the mechanism of the hydrogen transfer reactions of a vitamin E analogue to determine whether the reaction between **1H** and DPPH$^\bullet$ or G$^\bullet$ proceeds *via* a one-step hydrogen atom transfer or *via* electron transfer.

Experimental

Materials

2,2,5,7,8-Pentamethylchroman-6-ol (**1H**) was purchased from Wako Pure Chemical Ind. Ltd., Japan. 2,2-Bis(4-*tert*-octylphenyl)-1-picrylhydrazyl (DPPH$^\bullet$) and galvinoxyl (G$^\bullet$) were obtained commercially from Aldrich. Mg(ClO$_4$)$_2$ and acetonitrile (MeCN; spectral grade) were purchased from Nacalai Tesque, Inc., Japan and used as received.

Spectral and kinetic measurement

Typically, an aliquot of **1H** (2.0×10^{-2} M) in deaerated MeCN was added to a quartz cuvette (10 mm i.d.) which contained DPPH$^\bullet$ (1.4×10^{-5} M) in deaerated MeCN (3.0 ml). This led to a hydrogen-transfer reaction from **1H** to DPPH$^\bullet$. UV–VIS spectral changes associated with this reaction were monitored using a Hewlett-Packard 8453 photo diode array spectrophotometer. The rates of hydrogen transfer were determined by monitoring the absorbance change at 543 nm due to DPPH$^\bullet$ ($\varepsilon = 1.18 \times 10^4$ dm^3 mol^{-1} cm^{-1}). Pseudo-first-order or second-order rate constants were determined by a least-squares curve fit using an Apple Macintosh personal computer. The first-order plots of ln($A_\infty - A$) *vs.* time and the second-order plots of ($A_\infty - A$)$^{-1}$ *vs.* time (A_∞ and A refer to the final absorbance and the absorbance at the reaction time, respectively) were linear until three or more half-lives with the correlation coefficient $\rho >$ 0.999. The reaction of **1H** with G$^\bullet$ was carried out in the same manner and the rates were determined from the absorbance change at 428 nm due to G$^\bullet$ ($\varepsilon = 1.43 \times 10^5$ dm^3 mol^{-1} cm^{-1}).

EPR measurements

Typically, an aliquot of a stock solution of **1H** (1.0×10^{-3} M) was added to a LABOTEC LLC-04B EPR sample tube containing a deaerated MeCN solution of DPPH$^\bullet$ (1.0×10^{-3} M) in the presence or absence of 0.1 M Mg(ClO$_4$)$_2$ under an atmospheric pressure of Ar. EPR spectra of the phenoxyl radical **1$^\bullet$** produced in the reaction between **1H** and DPPH$^\bullet$ were taken on a JEOL X-band spectrometer (JES-FA100). The EPR spectra were recorded under nonsaturating microwave power conditions. The magnitude of modulation was chosen to optimize the resolution and the signal-to-noise (S/N) ratio of the observed spectra. The g values and the hyperfine coupling constants were calibrated with a Mn^{2+} marker. Computer simulation of the EPR spectra was carried out using Calleo ESR Version 1.2 program (Calleo Scientific Publisher) on an Apple Macintosh personal computer.

Cyclic voltammetry

The cyclic voltammetry measurements were performed on a BAS 100 W electrochemical analyzer in deaerated MeCN containing 0.10 M NBu$_4$ClO$_4$ as a supporting electrolyte. The Pt working electrode (BAS) was polished with BAS polishing alumina suspension and rinsed with acetone before use. The counter electrode was a platinum wire. The measured potentials were recorded with respect to an Ag/AgNO$_3$ (0.01 M) reference electrode. The $E_{1/2}$ values (*vs.* Ag/AgNO$_3$) were converted to

those *vs.* SCE by adding 0.29 V.[30] All electrochemical measurements were carried out at 298 K under an atmospheric pressure of argon.

Theoretical calculations

Density functional calculations were performed on a COMPAQ DS20E computer using the Amsterdam Density Functional (ADF) program version 1999.02 developed by Baerends *et al.*[31] The electronic configurations of the molecular systems were described by an uncontracted triple-ζ Slater-type orbital basis set (ADF basis set IV) with a single polarization function used for each atom. Core orbitals were frozen through 1s (C, O) and 2p (Mg). The calculations were performed using the local exchange-correlation potential by Vosko *et al.*[32] and the nonlocal gradient corrections by Becke[33] and Perdew[34] during the geometry optimizations. First-order scalar relativistic correlations were added to the total energy. Final geometries and energetics were optimized by using the algorithm of Versluis and Ziegler[35] provided in the ADF package and were considered converged when the changes in bond lengths between subsequent iterations fell below 0.01 Å.

Results and discussion

Stabilization of phenoxyl radical of a vitamin E analogue by magnesium ion

When **1H** was added to a deaerated acetonitrile (MeCN) solution of DPPH$^\bullet$, the visible absorption band at 543 nm due to DPPH$^\bullet$ immediately decreased, accompanied by an increase in the absorption bands at 402 and 423 nm with clear isosbestic points at 343, 374, and 437 nm as shown in Fig. 1. The absorp-
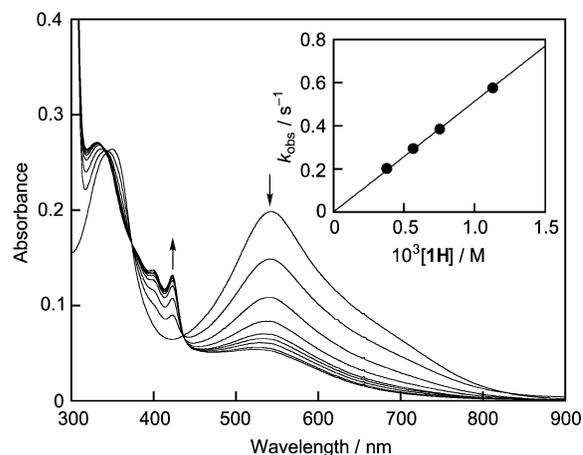

Fig. 1 Spectral changes in the reaction of **1H** (7.5×10^{-4} M) with DPPH$^\bullet$ (1.4×10^{-5} M) in deaerated MeCN at 298 K (2 s interval). Inset: Plot of k_{obs} *vs.* [**1H**].

tion bands around 400 nm and the broad band around 530 nm are typical for phenoxyl radical species of α-tocopherol.[36] This indicates that hydrogen atom transfer from **1H** to DPPH$^\bullet$ occurs to produce the corresponding phenoxyl radical **1$^\bullet$** and DPPH$_2$ [eqn. (1)]. In fact, the EPR spectrum having a g value of 2.0047 due to **1$^\bullet$** was observed in the reaction of **1H** with DPPH$^\bullet$ in deaerated MeCN at 298 K as shown in Fig. 2(a). The EPR signal of **1$^\bullet$** gradually decreased with prolonged reaction time.[37] The observed hyperfine structure in Fig. 2(a) is well reproduced by the computer simulation with the hyperfine splitting (hfs) values of one set of methylene protons (1.39 G) and three sets of methyl protons (5.87, 4.40 and 0.86 G). Based on the reported hfs values for **1$^\bullet$** in benzene[37d] as well as the calculated spin density of **1$^\bullet$** by the Amsterdam Density Functional (ADF) method (see Experimental section), we assigned those hfs values as shown in Table 1.

Table 1 g Values and hyperfine splitting (hfs) values (in G) of **1·** and Mg^{2+}-**1·** in deaerated MeCN

Radical	g	$a(3H^5)$	$a(3H^7)$	$a(3H^8)$	$a(2H^4)$
1·	2.0047	5.87	4.40	0.86	1.39
1·[a]	2.00476[a]	6.04[a]	4.55[a]	0.96[a]	1.48[a]
Mg^{2+}-**1·**	2.0040	3.35	—	4.86	—

[a] Taken from ref 37d (in benzene).
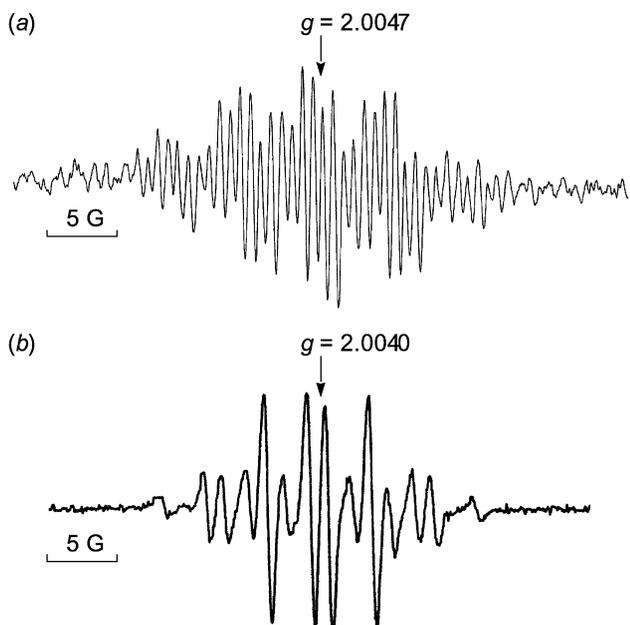
Fig. 2 (a) EPR spectrum of **1·** generated in the reaction of **1H** (1.0×10^{-3} M) with DPPH· (1.0×10^{-3} M) in deaerated MeCN at 298 K; (b) EPR spectrum of the Mg^{2+}–**1·** complex generated in the reaction of **1H** (1.0×10^{-3} M) with DPPH· (1.0×10^{-3} M) in the presence of 0.1 M Mg(ClO$_4$)$_2$ in deaerated MeCN at 298 K.
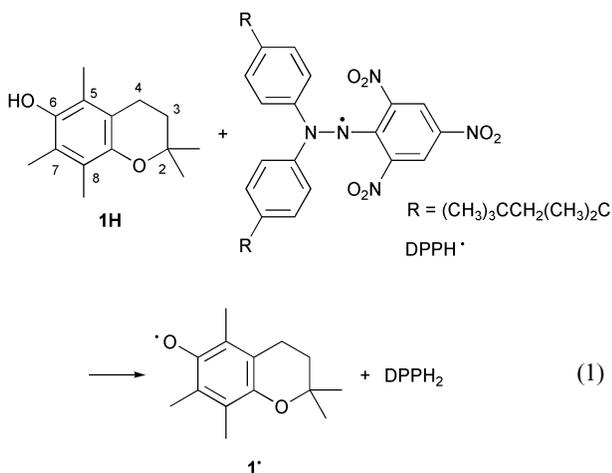
The decrease in the absorbance at 543 nm due to DPPH· obeyed pseudo-first-order kinetics under conditions where the concentration of **1H** was maintained at more than a 10-fold excess of DPPH· concentration. The pseudo-first-order rate constant (k_{obs}) increases linearly with an increase in concentration of **1H** as shown in the inset of Fig. 1. From the slope of the linear plot of k_{obs} vs. [**1H**] the second-order rate constant for hydrogen transfer (k_{HT}) from **1H** to DPPH· was obtained as 5.1×10^2 M^{-1} s^{-1}. This value is nearly the same as the k_{HT} value (4.9×10^2 M^{-1} s^{-1}) reported for hydrogen transfer from α-tocopherol to DPPH· in MeCN.[38] When DPPH· was replaced by the galvinoxyl radical (G·), the decay of the absorption band at 428 nm due to G· was observed upon addition of **1H** to a deaerated MeCN solution of G·. Such spectral change can be

ascribed to a hydrogen atom transfer from **1H** to G· [eqn. (2)]. The rate constant for hydrogen transfer from **1H** to G· was determined in the same manner as in the case of DPPH· as 3.0×10^3 M^{-1} s^{-1}, which is about 6-fold larger than that determined for DPPH·. Although the absorption bands at 402 and 423 nm due to **1·** generated by hydrogen transfer from **1H** to G· could not be observed because of the overlap with the large absorption band at 428 nm due to G·, the formation of **1·** can be confirmed from its EPR spectrum.
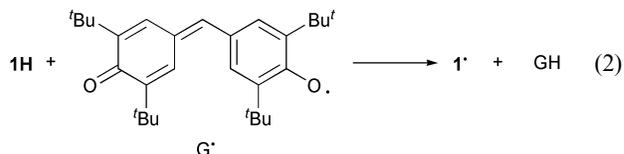
The phenoxyl radical (**1·**) generated by hydrogen transfer from **1H** to DPPH· gradually decomposed at room temperature (Fig. 3(a)).[36] The decrease in the absorption band at 423 nm due
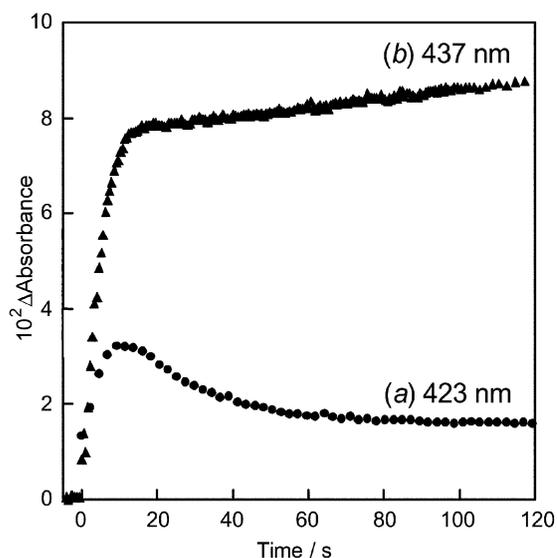
Fig. 3 (a) Time course of the absorption change at 423 nm due to **1·** (black circles) in the reaction of **1H** (7.5×10^{-4} M) with DPPH· (1.4×10^{-5} M) in deaerated MeCN at 298 K. (b) Time course of the absorption change at 437 nm due to the Mg^{2+}-**1·** complex (black triangles) in the reaction of **1H** (7.5×10^{-4} M) with DPPH· (1.4×10^{-5} M) in the presence of 0.1 M Mg(ClO$_4$)$_2$ in deaerated MeCN at 298 K.

to **1·** obeys second-order kinetics in agreement with the decay occurring via a bimolecular disproportionation reaction to give **1H** and the corresponding quinone methide (**2**) as shown in Scheme 1.[29,36] The second-order rate constant (k_{dec}) for
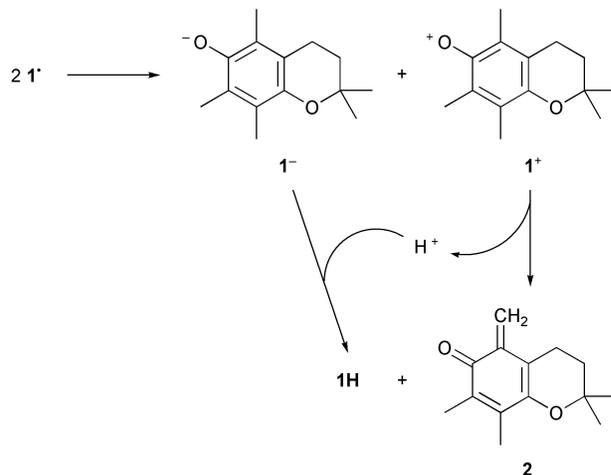
Scheme 1

the decomposition of **1·** in deaerated MeCN at 298 K was determined from the second-order plot as 2.7×10^3 M^{-1} s^{-1}.[39]

In the presence of Mg(ClO$_4$)$_2$ (0.1 M), the reaction between **1H** and DPPH· also took place to give the phenoxyl radical species in deaerated MeCN, the absorption bands of which, however, were shifted from 402 and 423 nm to 412 and 437 nm, respectively. It should be noted that no decay of these absorption bands was observed, demonstrating significantly the enhanced stability of the phenoxyl radical species in the presence of Mg(ClO$_4$)$_2$ (Fig. 3(b)). Since the disproportionation reaction between the two molecules of **1·** involves both oxidation and reduction, **1·** must act as both the oxidant and reductant (Scheme 1).[29] Although the complexation of the Lewis acid such as Mg^{2+} with **1·** would accelerate the reduction of **1·** to the phenolate **1⁻**, it would decelerate the oxidation process due to the repulsive interaction between the oxidized product **1⁺** and Mg^{2+} at the same time.[29] Thus, the destabilization of **1⁺** by Mg^{2+} governs the overall reactivity in the disproportionation reaction to stabilize the phenoxyl radical species **1·** in the presence of Mg^{2+}.

Effects of magnesium ion on the spin distribution of the phenoxyl radical

The EPR spectrum of the Mg^{2+} complex of **1·** generated in the reaction of **1H** with DPPH· in the presence of 0.1 M Mg(ClO$_4$)$_2$ in deaerated MeCN is observed as shown in Fig. 2(b). The g value of the EPR spectrum of Mg^{2+}–**1·** is determined as 2.0040, which is appreciably smaller than the g value of **1·** (2.0047). The smaller g value of Mg^{2+}–**1·** (2.0040) than that of **1·** (2.0047) indicates that the spin density on oxygen nuclei in Mg^{2+}–**1·** is decreased by complexation with Mg^{2+}–**1·**.[29] The hyperfine structure can be reproduced by computer simulation with the hyperfine splitting (hfs) values of two sets of methyl protons (4.86 and 3.35 G). As in the case of **1·**, we assigned those hfs values as shown in Table 1 based on the calculated spin density of Mg^{2+}–**1·** by the ADF method (see Experimental section).

It is interesting to note that the spin density at C(8) of Mg^{2+}–**1·** ($\rho = 0.094$) calculated using the ADF method is larger than that at C(5) ($\rho = 0.038$) (see Supplementary Fig. S(1b)†), while a relatively large amount of the spin density is accumulated at the C(5) and C(7) positions in **1·** (Fig. S(1a)). The same EPR spectrum of Mg^{2+}–**1·** was obtained for the **1H**–G·–Mg^{2+} system. No interaction between Mg^{2+} and DPPH· or G· has been detected in the electronic spectra as well as in the g values and hyperfine splitting constants of the EPR spectra of DPPH· or G· in the presence of Mg^{2+}. No change in the absorption spectra was observed either upon addition of Mg^{2+} to **1H**.

Effects of magnesium ion on the rate of hydrogen transfer

No effect of Mg^{2+} on the k_{HT} values of the hydrogen-transfer reaction of **1H** was observed in the case of DPPH· or G· used as a hydrogen abstracting agent (see Supplementary Fig. S(2)†). Thus, there may be no contribution of electron transfer from **1H** to DPPH· or G· in the hydrogen-transfer reaction, which may thereby proceed *via* a one-step hydrogen-transfer process.[28] If the hydrogen transfer from **1H** to DPPH· or G· involves an electron-transfer process as the rate-determining step, the rate of hydrogen transfer would be accelerated by the presence of Mg^{2+} which is known to accelerate the electron transfer to DPPH· and G·.[28]

Judging from the one-electron oxidation potential of **1H** (E^0_{ox} *vs.* SCE = 0.77 V) which is higher than the one-electron reduction potential of DPPH· (E^0_{red} *vs.* SCE = 0.18 V) or G· (E^0_{red} *vs.* SCE = 0.05 V), the free energy change of electron transfer from **1H** to DPPH· or G· is positive [ΔG^0_{et}(in eV) = $e(E^0_{ox} - E^0_{red}) > 0$, where e is the elementary charge], and thereby the electron-transfer step is endergonic. In such a case, the overall rate of hydrogen transfer (k_{HT}) which consists of
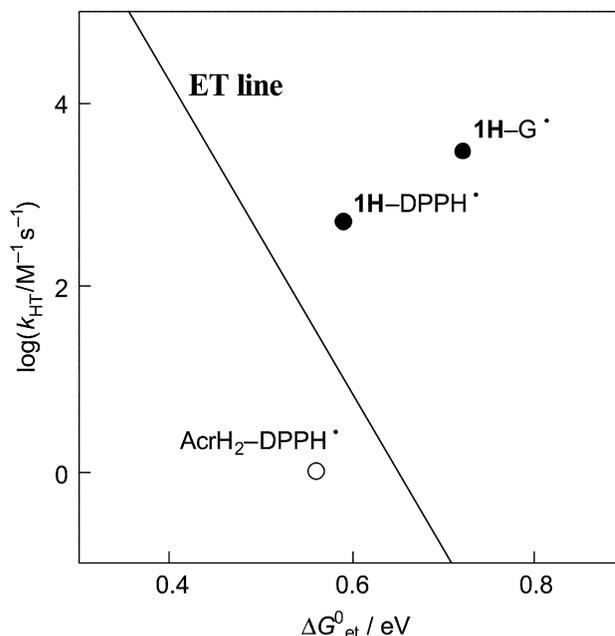

Fig. 4 Plot of the rate constant of hydrogen transfer from **1H** or AcrH$_2$ to DPPH· or G· (logk_{HT}) *vs.* the free energy of electron transfer from **1H** or AcrH$_2$ to DPPH· or G· (ΔG^0_{et}). The solid line shows the dependence of the calculated rate constant of electron transfer (k_{et}) on ΔG^0_{et} based on eqn. (3), see text.

electron-transfer and proton-transfer steps would be slower than the initial electron-transfer rate (k_{et}). The maximum k_{et} value is evaluated from the ΔG^0_{et} value by eqn. (3), where Z is the frequency factor taken as 1×10^{11} M^{-1} s^{-1},[40] and k_B is the Boltzmann constant.

$$k_{et} = Z\exp(-\Delta G^0_{et}/k_B T) \qquad (3)$$

Fig. 4 shows a plot of log k_{HT} *versus* ΔG^0_{et}, calculated by eqn. (3) (denoted by the ET line). The k_{HT} values of both the **1H**–DPPH· and **1H**–G· systems (black circles) are significantly above the ET line. The k_{HT} value of the **1H**–DPPH· system as well as that of the **1H**–G· system, which is much larger than the corresponding k_{et} value, indicates that the hydrogen transfer proceeds *via* a direct one-step hydrogen transfer rather than *via* electron transfer. In such a case, no effect of Mg^{2+} on the k_{HT} values should be observed, as is confirmed experimentally.

On the other hand, the hydrogen transfer from an NADH analogue, 10-methyl-9,10-dihydroacridine (AcrH$_2$) (E^0_{ox} = 0.81 V *vs.* SCE)[41] to DPPH· has been reported to proceed *via* electron transfer from AcrH$_2$ to DPPH·, which is accelerated by the presence of Mg^{2+}, followed by proton transfer from AcrH$_2^{·+}$ to DPPH⁻ to yield the acridinyl radical (AcrH·) and DPPH$_2$.[28] The resulting AcrH· is a much stronger reductant than AcrH$_2$, judging from the negative oxidation potential (E^0_{ox} = − 0.43 V)[28] as compared to that of AcrH$_2$ (0.81 V),[41] and thereby AcrH· can readily transfer an electron to another DPPH· molecule to yield AcrH⁺ (Scheme 2).[28] In such a case, the k_{HT} value (white circle in Fig. 4), which is much smaller than the corresponding maximum k_{et} value, indicates that the hydrogen transfer proceeds *via* electron transfer followed by proton transfer.

In conclusion, the phenoxyl radical of the vitamin E analogue **1H** generated by hydrogen atom transfer from **1H** to DPPH· or G· is significantly stabilized by Mg^{2+} by complexation of **1·** with Mg^{2+} as shown in Scheme 3.

No effect of Mg^{2+} on the hydrogen transfer rate from **1H** to DPPH· or G· indicates that the hydrogen-transfer reaction from **1H** to DPPH· or G· proceeds *via* a one-step hydrogen-transfer process rather than *via* electron transfer.
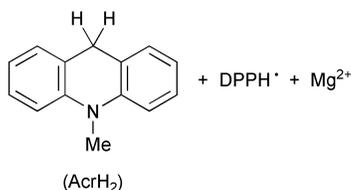
Scheme 2
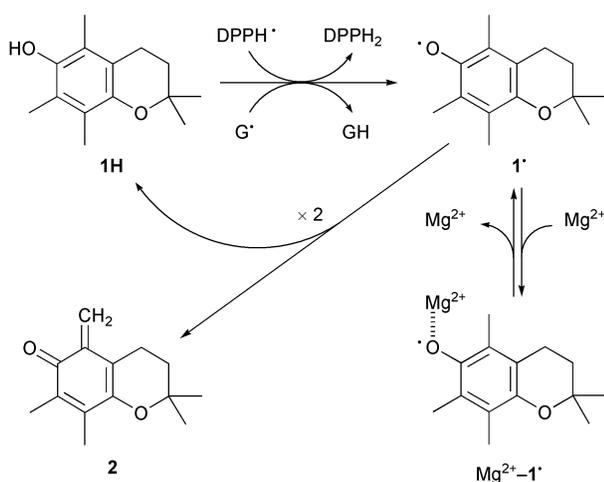
Scheme 3

Acknowledgements

References

1 L. J. Machlin, in *Hand Book of Vitamins*, ed. L. J. Machlin, Marchel Dekker, New York, 2nd edn., 1991, pp. 99–144.
2 C. K. Chow, *Free Radical Biol. Med.*, 1991, **11**, 215.
3 G. W. Burton and K. U. Ingold, *Acc. Chem. Res.*, 1986, **19**, 194.
4 C. Suarna, D. C. Craig, K. J. Cross and P. T. Southwell-Keely, *J. Org. Chem.*, 1988, **53**, 1281.
5 M. Matsuo, S. Matsumoto and T. Ozawa, *Org. Magn. Reson.*, 1983, **21**, 261.
6 T. Doba, G. W. Burton and K. U. Ingold, *J. Am. Chem. Soc.*, 1983, **105**, 6505.
7 G. W. Burton, T. Doba, E. Gaba, L. Hughes, F. L. Lee, L. Prasad and K. U. Ingold, *J. Am. Chem. Soc.*, 1985, **107**, 7053.
8 S. Urano, S. Yamanoi, Y. Hattori and M. Matsuo, *Lipids*, 1977, **12**, 105.
9 W. A. Skinner and P. Alaupovic, *J. Org. Chem.*, 1963, **28**, 2854.
10 H. Meerwein, *Angew. Chem.*, 1955, **67**, 374.
11 K. Dimroth, W. Umbach and H. Thomas, *Chem. Ber.*, 1967, **100**, 132.
12 P. D. Boyer, *J. Am. Chem. Soc.*, 1951, **73**, 733.
13 W. Durckheimer and L. A. Cohen, *J. Am. Chem. Soc.*, 1964, **86**, 4388.
14 C. Martius and H. Eilingsfeld, *Liebigs Ann. Chem.*, 1957, **607**, 159.
15 W. John, E. Dietzel and W. Emte, *Z. Physiol. Chem.*, 1939, **257**, 173.
16 W. A. Skinner and R. M. Parkhurst, *J. Org. Chem.*, 1966, **31**, 1248.
17 J. L. G. Nilsson, J. O. Branstad and H. Sievertsson, *Acta Pharm. Suec.*, 1968, **5**, 509.
18 D. R. Nelan and C. D. Robeson, *J. Am. Chem. Soc.*, 1962, **84**, 2963.
19 M. Jujimaki, K. Kanamaru, T. Kurata and O. Igarashi, *Agric. Biol. Chem.*, 1970, **34**, 1781.
20 V. L. Frampton, W. A. Skinner, P. Cambour and P. S. Bailey, *J. Am. Chem. Soc.*, 1960, **82**, 4632.
21 F. M. Dean, K. B. Hindley, L. E. Houghton and M. L. Robinson, *J. Chem. Soc., Perkin Trans. 1*, 1976, 600.
22 S. Fukuzumi, in *Advances in Electron Transfer Chemistry*, ed. P. S. Mariano, JAI Press, Greenwich, 1992, vol. 2, pp. 67–175; and refs. cited therein.
23 (*a*) D. Mauzerall and F. H. Westheimer, *J. Am. Chem. Soc.*, 1955, **77**, 2261; (*b*) R. H. Abeles, R. F. Hutton and F. H. Westheimer, *J. Am. Chem. Soc.*, 1957, **79**, 712.
24 (*a*) E. M. Kosower, in *Free Radicals in Biology*, ed. W. A. Pryor, Academic Press, New York, 1976, vol. II, ch. 1; (*b*) S. Fukuzumi and T. Tanaka, in *Photoinduced Electron Transfer*, ed. M. A. Fox and M. Chanon, Elsevier, Amsterdam, 1988, Part C, ch. 10.
25 U. Svanholm, K. Bachgaard and V. Parker, *J. Am. Chem. Soc.*, 1974, **96**, 2409.
26 G. W. Burton, T. Doba, E. J. Gabe, L. Hughes, F. L. Lee, L. Prasad and K. U. Ingold, *J. Am. Chem. Soc.*, 1985, **107**, 7053.
27 (*a*) K. Mukai, K. Fukuda, K. Tajima and K. Ishizu, *J. Org. Chem.*, 1988, **53**, 430; (*b*) K. Mukai, Y. Kageyama, T. Ishida and K. Fukuda, *J. Org. Chem.*, 1989, **54**, 552.
28 S. Fukuzumi, Y. Tokuda, Y. Chiba, L. Greci, P. Carloni and E. Damiani, *J. Chem. Soc., Chem. Commun.*, 1993, 1575.
29 S. Itoh, H. Kumei, S. Nagatomo, T. Kitagawa and S. Fukuzumi, *J. Am. Chem. Soc.*, 2001, **123**, 2165.
30 K. Mann and K. K. Barnes, in *Electrochemical Reactions in Nonaqueous Systems*, Marcel Dekker Inc., New York, 1990.
31 (*a*) E. J. Baerends, D. E. Ellis and P. Ros, *Chem. Phys.*, 1973, **2**, 41; (*b*) G. te Velde and E. J. Baerends, *J. Comput. Phys.*, 1992, **99**, 84.
32 S. H. Vosko, L. Wilk and M. Nusair, *Can. J. Phys.*, 1980, **58**, 1200.
33 A. Becke, *Phys. Rev. A*, 1988, **38**, 3098.
34 (*a*) J. P. Perdew, *Phys. Rev. B*, 1986, **33**, 8822; (*b*) J. P. Perdew, *Phys. Rev. B*, 1986, **34**, 7406.
35 L. Versluis and T. Ziegler, *J. Chem. Phys.*, 1988, **88**, 322.
36 V. W. Bowry and K. U. Ingold, *J. Org. Chem.*, 1995, **60**, 5456.
37 For the EPR spectrum of the phenoxyl radical derived from α-tocopherol and its analogues, see (*a*) R. J. Singh, S. P. A. Goss, J. Joseph and B. Kalyanaraman, *Proc. Natl. Acad. Sci. USA*, 1998, **95**, 12912; (*b*) B. Kalyanaraman, V. M. Darley-Usmar, J. Wood, J. Joseph and S. Parthasarathy, *J. Biol. Chem.*, 1992, **267**, 6789; (*c*) B. Kalyanaraman, W. E. Antholine and S. Parthasarathy, *Biochim. Biophys. Acta*, 1990, **1035**, 286; (*d*) G. W. Burton, T. Doba, E. J. Gabe, L. Hughes, F. L. Lee, L. Prasad and K. U. Ingold, *J. Am. Chem. Soc.*, 1985, **107**, 7053; (*e*) J. Tsuchiya, E. Niki and Y. Kamiya, *Bull. Chem. Soc. Jpn.*, 1983, **56**, 229; (*f*) W. Boguth and H. Niemann, *Biochim. Biophys. Acta*, 1971, **248**, 121.
38 L. Valgimigli, J. T. Banks, K. U. Ingold and J. Lusztyk, *J. Am. Chem. Soc.*, 1995, **117**, 9966.
39 The second-order decomposition rate constant for α-TO· in chlorobenzene at 296 K is reported as 3.9×10^3 M^{-1} s^{-1}. See ref. 36 and refs cited therein.
40 (*a*) R. A. Marcus, *Annu. Rev. Phys. Chem.*, 1964, **15**, 155; (*b*) R. A. Marcus, *Angew. Chem., Int. Ed. Engl.*, 1993, **32**, 1111.
41 S. Fukuzumi, Y. Tokuda, T. Kitano, T. Okamoto and J. Otera, *J. Am. Chem. Soc.*, 1993, **115**, 8960.